Steel and Composite Structures, *Vol. 19, No. 3 (2015) 713-733*
DOI: http://dx.doi.org/10.12989/scs.2015.19.3.713

Viscous fluid induced vibration and instability of FG-CNT-reinforced cylindrical shells integrated with piezoelectric layers

Mahmood Rabani Bidgoli [*1], Mohammad Saeed Karimi [1] and Ali Ghorbanpour Arani [2,3]

[1] *Faculty of Civil Engineering, Semnan University, Semnan, Iran*
[2] *Faculty of Mechanical Engineering, University of Kashan, Kashan, Iran*
[3] *Institute of Nanoscience & Nanotechnology,University of Kashan, Kashan, Iran*

(*Received November 11, 2014, Revised February 28, 2015, Accepted March 04, 2015*)

Abstract. In this paper, viscous fluid induced nonlinear free vibration and instability analysis of a functionally graded carbon nanotube-reinforced composite (CNTRC) cylindrical shell integrated with two uniformly distributed piezoelectric layers on the top and bottom surfaces of the cylindrical shell are presented. Single-walled carbon nanotubes (SWCNTs) are selected as reinforcement and effective material properties of FG-CNTRC cylindrical shell are assumed to be graded through the thickness direction and are estimated through the rule of mixture. The elastic foundation is modeled by temperature-dependent orthotropic Pasternak medium. Considering coupling of mechanical and electrical fields, Mindlin shell theory and Hamilton's principle, the motion equations are derived. Nonlinear frequency and critical fluid velocity of sandwich structure are calculated based on differential quadrature method (DQM). The effects of different parameters such as distribution type of SWCNTs, volume fractions of SWCNTs, elastic medium and temperature gradient are discussed on the vibration and instability behavior of the sandwich structure. Results indicate that considering elastic foundation increases frequency and critical fluid velocity of system.

Keywords: nonlinear vibration; viscous fluid; FG-CNTRC; piezoelectric layers; DQM

1. Introduction

Piezoelectric coupled cylindrical shells are one of the key components in smart structures due to their electromechanical coupling characteristics. Smart structures are widely used as sensors and actuators in various engineering applications, including passive/semi-active/active vibration control, acoustic noise suppression, shape control, active damping and health monitoring of engineering structures. Piezoelectric actuators in the form of discs or rings were employed to produce motion in circular/ annular plates used in micro-pumps and micro-valves (Spencer *et al*. 1978, Dong *et al*. 2002), in devices for generating and detecting sounds (Chee *et al*. 1998), in implantable medical devices (Cao *et al*. 2001), and in microswitches with piezoelectric-film actuation (Chen *et al*. 2004). Due to their wide range of applications, accurate natural frequencies of smart cylindrical shells must be known to achieve an appropriate design.

The coupling effect existing between the elastic and electric fields in piezoelectric materials has

*Corresponding author, Ph.D., E-mail: m.rabanibidgoli@gmail.com

http://www.techno-press.org/?journal=scs&subpage=8 ISSN: 1229-9367 (Print), 1598-6233 (Online)

been used in various engineering applications. There are two characteristics of piezoelectric materials which permit them to be used as sensors and actuators. One is their direct effect which implies that the materials induce electric charge or electric potential when they are subjected to external mechanical deformations. Conversely, they are deformed if some electric charge or electric potential is imposed on them. Literature dealing with research on the behaviour of electro-elastic structures has gained more importance recently as these smart or intelligent materials have ability of converting energy from electric to mechanical, or conversely. The early investigations of elasto-electric characteristic for composite cylindrical shells are reviewed in the following. Lester and Lefebvre (1991) investigated the coupling between the cylindrical mode and internal acoustic cavity modes using modal spectra and proved theoretically that the piezoelectric actuator can be used for internal cavity noise control. Clark and Fuller (1991) carried out acoustic control experiments using a piezoceramic actuator, microphone, PVDF sensor mounted on an aluminum shell and the Filtered-xL MS control technique. Siao *et al*. (1994) presented a finite element method for determining the vibration characteristic of a circular cylinder composed of bounded piezoelectric layers. The finite element modeling occurs in the radial direction only using quadratic polynomials. Lu *et al*. (2001) presented an approach for investigating vibration characteristics of piezoelectric cylindrical shells under transverse vibration modes. Based on a previous work for elastic shells they developed a formula to estimate the transverse frequencies of the piezoelectric cylindrical shells. Bending and free vibration of multilayered cylindrical shells with piezoelectric properties using a semi-analytical axisymetric shell finite element model with piezoelectric layers using the 3D linear elasticity was depicted by Santos *et al*. (2008). Free vibration of piezoelectric laminated cylindrical shells under a hydrostatic pressure by making the use of Hamilton's principle nonlinear dynamic equation by Li *et al*. (2001). On the basis of the piezoelectric equations and wave equations, with ignoring the shearing strain, the three-dimensional coupled vibration of the longitudinally polarized piezoelectric ceramic hollow cylinder whose height and thickness are comparable with its radius is studied analytically by Lin (2004). Vel and Baillargeon (2005) presented an analytical solution for the static deformation and steady-state vibration of simply supported cylindrical shells consisting of fiber-reinforced layers with embedded piezoelectric shear sensors and actuators. Suitable displacement and electric potential functions that identically satisfy the boundary conditions at the simply supported edges are used to reduce the governing equations of static deformation and steady-state vibrations. Free vibration problem of multilayered shells with embedded piezoelectric materials was discussed by D'Ottavio *et al*. (2006) by using a series of hierarchic, two-dimensional axiomatic shell theories which are presented within the ''unified formulation". Chen *et al*. (2006) developed three-dimensional state space analysis for a simply supported, cross-ply piezoelectric laminated cylindrical panel with inter laminar bonding imperfections by using a layer wise method. Sohn *et al*. (2006) analyzed the natural vibration characteristics of the cylindrical shell equipped with an MFC actuator using the finite element code and proved theoretically that the LQG controller could be used as an active vibration controller. Dynamic modeling, active vibration controller design and experiments for a cylindrical shell equipped with piezoelectric sensors and actuators were presented by Moon *et al*. (2009). Free vibration analysis of laminated cylindrical shell with integrated surfaces piezoelectric layers with arbitrary edges condition based on 3D theory of elasticity and using DQ in conjunction with state space method has not been considered yet.

In the present study, nonlinear vibration and instability of piezoelectric sandwich cylindrical shells conveying viscous fluid resting on temperature-dependent orthotropic Pasternak medium are investigated. The nonlinear formulation is based on the first-order shear deformation shell theory

and the Von Kármán assumption accounting for transverse shear strains, rotary inertia and moderate rotations. Two kinds of CNTRC cylindrical shell, namely, UD and FG distributions of the reinforcement are considered in middle layer. The material properties of FG-CNTRCs are assumed to be graded in the thickness direction and are estimated through the rule of mixture. Frequency and critical fluid velocity of sandwich structure are obtained using DQM. The effects of the volume fractions of CNT, Pasternak medium, temperature and CNTs patterns on the frequency and critical fluid velocity of the system are disused in detail.

2. Rule of mixture

As shown in Fig. 1, a CNTRC cylindrical shell integrated with piezoelectric layers is considered. The sandwich structure is surrounded by an orthotropic Pasternak medium which is simulated by K_W, $K_{g\xi}$ and $K_{g\eta}$ correspond Winkler foundation parameter, shear foundation parameters in ξ and η directions, respectively.

Four types of CNTRC cylindrical shell namely as uniform distribution (UD) along with three types of FG distributions (FGA, FGO, FGX) of CNTs along the thickness direction of a CNTRC cylindrical shell are considered. In order to obtain the equivalent material properties two-phase nanocomposites (i.e., polymer as matrix and CNT as reinforcer), the rule of mixture (Esawi and Farag 2007) is applied. According to mixture rule, the effective Young and shear moduli of CNTRC cylindrical shell can be written as

$$E_{11} = \eta_1 V_{CNT} E_{r11} + (1 - V_{CNT}) E_m, \tag{1}$$

$$\frac{\eta_2}{E_{22}} = \frac{V_{CNT}}{E_{r22}} + \frac{(1 - V_{CNT})}{E_m}, \tag{2}$$

$$\frac{\eta_3}{G_{12}} = \frac{V_{CNT}}{G_{r12}} + \frac{(1 - V_{CNT})}{G_m}, \tag{3}$$

where E_{r11}, E_{r22} and G_{r11} indicate the Young's moduli and shear modulus of SWCNTs, respectively; E_m, G_m represent the corresponding properties of the isotropic matrix; η_j is called the CNT efficiency parameter; V_{CNT} and V_m are the volume fractions of the CNTs and matrix, respectively. The uniform and three types of FG distributions of the CNTs along the thickness direction of the CNTRC cylindrical shells take the following forms

$$UD: \quad V_{CNT} = V_{CNT}^*, \tag{4}$$

$$FGV: \ V_{CNT}(z) = \left(1 - \frac{2z}{h}\right) V_{CNT}^*, \tag{5}$$

$$FGO: \ V_{CNT}(z) = 2\left(1 - \frac{2|z|}{h}\right) V_{CNT}^*, \tag{6}$$

$$FGX: \ V_{CNT}(z) = 2\left(\frac{2|z|}{h}\right)V_{CNT}^{*}, \tag{7}$$

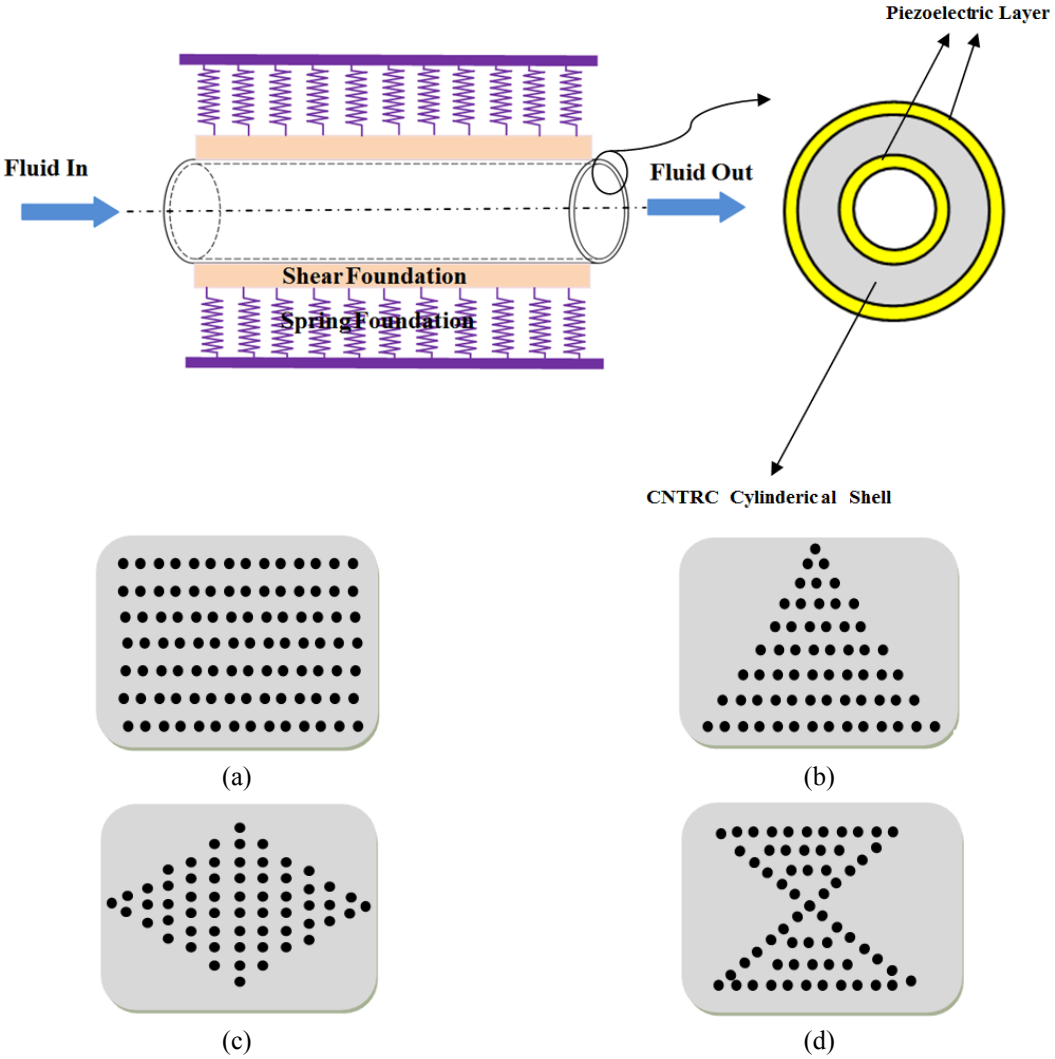

Fig. 1 Configurations of the SWCNT distribution in a sandwich structure. (a) UD; (b) FGA; (c) FGO; (d) FGX

where

$$V_{CNT}^{*} = \frac{w_{CNT}}{w_{CNT} + (\rho_{CNT}/\rho_m) - (\rho_{CNT}/\rho_m)w_{CNT}}, \tag{8}$$

where w_{CNT}, ρ_m and ρ_{CNT} are the mass fraction of the CNT, the densities of the matrix and CNT, respectively. Similarly, the thermal expansion coefficients in the longitudinal and transverse directions respectively (α_{11} and α_{22}), Poisson's ratio (ν_{12}) and the density (ρ_s) of the CNTRC

cylindrical shell can be determined as

$$\nu_{12} = V_{CNT}^{*}\nu_{r12} + V_{m,}\nu_{m}, \tag{9}$$

$$\rho_{s} = V_{CNT}^{*}\rho_{r} + V_{m,}\rho_{m,}, \tag{10}$$

$$\alpha_{11} = V_{CNT}^{*}\alpha_{r11} + V_{m,}\alpha_{m,}, \tag{11}$$

$$\alpha_{22} = (1+\nu_{r12})V_{CNT}\alpha_{r22} + (1+\nu_{m})V_{m}\alpha_{m} - \nu_{12}\alpha_{11}, \tag{12}$$

where v_{r12} and v_m are Poisson's ratios of the CNT and matrix, respectively; α_{r11}, α_{r22} and α_m are the thermal expansion coefficients of the CNT and matrix, respectively. It should be noted that v_{12} is assumed as constant over the thickness of the FG-CNTRC cylindrical shells.

3. Mathematical modeling of system

3.1 Mindlin theory

In order to peruse physical behaviour of cylindrical shells in confront with lateral and in-plane forces, Mindlin theory of plates has been opted. Displacement filed corresponds to this theory is expressed as (Reddy 1984)

$$\begin{aligned} u_{x}(x,\theta,z,t) &= u\ (x,\theta,t) + z\psi_{x}(x,\theta,t), \\ u_{\theta}(x,\theta,z,t) &= v(x,\theta,t) + z\psi_{\theta}(x,\theta,t), \\ u_{z}(x,\theta,z,t) &= w(x,\theta,t), \end{aligned} \tag{13}$$

where (u_x, $u_{\theta i}$, u_z) denote the displacement components at an arbitrary point (x, θ, z) in the shell, and (u, v, w) are the displacement of a material point at (x, θ) on the mid-plane (i.e., z = 0) of the shell along the x-, θ-, and z-directions, respectively; ψ_x and $\psi_\theta$are the rotations of the normal to the mid-plane about x- and θ- directions, respectively.

The von Kármán strains associated with the above displacement field can be expressed in the following form

$$\begin{bmatrix} \varepsilon_{xx} \\ \varepsilon_{\theta\theta} \\ \gamma_{\theta z} \\ \gamma_{xz} \\ \gamma_{x\theta} \end{bmatrix} = \begin{bmatrix} \varepsilon_{xx}^{0} \\ \varepsilon_{\theta\theta}^{0} \\ \gamma_{\theta z}^{0} \\ \gamma_{xz}^{0} \\ \gamma_{x\theta}^{0} \end{bmatrix} + z\begin{bmatrix} \varepsilon_{xx}^{1} \\ \varepsilon_{\theta\theta}^{1} \\ \gamma_{\theta z}^{1} \\ \gamma_{xz}^{1} \\ \gamma_{x\theta}^{1} \end{bmatrix} = \begin{bmatrix} \dfrac{\partial u}{\partial x} + \dfrac{1}{2}\left(\dfrac{\partial w}{\partial x}\right)^{2} \\ \dfrac{\partial v}{R\partial\theta} + \dfrac{w}{R} + \dfrac{1}{2}\left(\dfrac{\partial w}{R\partial\theta}\right) \\ \dfrac{\partial w}{R\partial\theta} - \dfrac{v}{R} + \psi_{\theta} \\ \dfrac{\partial w}{\partial x} + \psi_{x} \\ \dfrac{\partial u}{R\partial\theta} + \dfrac{\partial v}{\partial x} + \dfrac{\partial w}{\partial x}\dfrac{\partial w}{R\partial\theta} \end{bmatrix} + z\begin{bmatrix} \dfrac{\partial \psi_{x}}{\partial x} \\ \dfrac{\partial \psi_{\theta}}{R\partial\theta} \\ 0 \\ 0 \\ \dfrac{\partial \psi_{x}}{R\partial\theta} + \dfrac{\partial \psi_{\theta}}{\partial x} \end{bmatrix}. \tag{14}$$

3.2 Constitutive equations

3.2.1 CNTRC Cylindrical shell

Constitutive equation of an orthotropic cylindrical shell is written as

$$\begin{Bmatrix}\sigma_{xx}\\ \sigma_{\theta\theta}\\ \sigma_{\theta z}\\ \sigma_{zx}\\ \sigma_{x\theta}\end{Bmatrix}=\begin{bmatrix}Q_{11}(z,T) & Q_{12}(z,T) & 0 & 0 & 0\\ Q_{21}(z,T) & Q_{22}(z,T) & 0 & 0 & 0\\ 0 & 0 & Q_{44}(z,T) & 0 & 0\\ 0 & 0 & 0 & Q_{55}(z,T) & 0\\ 0 & 0 & 0 & 0 & Q_{66}(z,T)\end{bmatrix}\begin{Bmatrix}\varepsilon_{xx}-\alpha_{xx}(z,T)\Delta T\\ \varepsilon_{\theta\theta}-\alpha_{\theta\theta}(z,T)\Delta T\\ \gamma_{\theta z}\\ \gamma_{xz}\\ \gamma_{x\theta}\end{Bmatrix}, \tag{15}$$

Noted that Q_{ij} and α_{xx}, $\alpha_{\theta\theta}$ may be obtained using rule of mixture (i.e., Eqs. (1)-(12)).

3.2.2 Piezoelectric layers

Constitutive equations correspond to piezoelectric layers are (Ghorbanpour Arani *et al*. 2013)

$$\begin{bmatrix}\sigma_{xx}^{P}\\ \sigma_{\theta\theta}^{P}\\ \sigma_{zz}^{P}\\ \sigma_{\theta z}^{P}\\ \sigma_{zx}^{P}\\ \sigma_{x\theta}^{P}\end{bmatrix}=\begin{bmatrix}C_{11} & C_{12} & C_{13} & 0 & 0 & 0\\ C_{12} & C_{11} & C_{13} & 0 & 0 & 0\\ C_{13} & C_{13} & C_{33} & 0 & 0 & 0\\ 0 & 0 & 0 & C_{44} & 0 & 0\\ 0 & 0 & 0 & 0 & C_{55} & 0\\ 0 & 0 & 0 & 0 & 0 & C_{66}\end{bmatrix}\begin{Bmatrix}\varepsilon_{xx}-\alpha_{xx}^{P}(T)\Delta T\\ \varepsilon_{\theta\theta}-\alpha_{\theta\theta}^{P}(T)\Delta T\\ \varepsilon_{zz}\\ \gamma_{\theta z}\\ \gamma_{zx}\\ \gamma_{x\theta}\end{Bmatrix}-\begin{bmatrix}e_{31} & 0 & 0\\ e_{31} & 0 & 0\\ e_{33} & 0 & 0\\ 0 & e_{15} & 0\\ 0 & 0 & e_{15}\\ 0 & 0 & 0\end{bmatrix}\begin{bmatrix}E_x\\ E_\theta\\ E_z\end{bmatrix}, \tag{16}$$

where C_{ij} are linear elastic constants and e_{31}, e_{33}, e_{15} are linear piezoelectric constants. Superscript P refers to piezoelectric material. E_i ($i = x, \theta, z$) shows electric filed intensity and can be obtained (Ghorbanpour Arani *et al*. 2014)

$$E_i=-\frac{\partial\phi}{\partial m},\quad m=x,\theta,z \tag{17}$$

where ϕ is applied electric potential to piezoelectric layers. On the other hand, electric displacement of piezoelectric material may be presented as (Ghorbanpour Arani *et al*. 2012)

$$\begin{bmatrix}D_{xx}\\ D_{\theta\theta}\\ D_{zz}\end{bmatrix}=\begin{bmatrix}e_{31} & e_{31} & e_{33} & 0 & 0 & 0\\ 0 & 0 & 0 & e_{15} & 0 & 0\\ 0 & 0 & 0 & 0 & e_{15} & 0\end{bmatrix}\begin{bmatrix}\varepsilon_{xx}-\alpha_{xx}^{P}(T)\Delta T\\ \varepsilon_{\theta\theta}-\alpha_{\theta\theta}^{P}(T)\Delta T\\ \varepsilon_{zz}\\ \gamma_{\theta z}\\ \gamma_{zx}\\ \gamma_{x\theta}\end{bmatrix}+\begin{bmatrix}K_{11} & 0 & 0\\ 0 & K_{11} & 0\\ 0 & 0 & K_{33}\end{bmatrix}\begin{bmatrix}E_x\\ E_\theta\\ E_z\end{bmatrix}, \tag{18}$$

in this equation, K_{11}, K_{33} are dielectric constants. In this investigation, electric field is applied along x direction and along two other directions considered zero. For our particular problem constitutive and electric displacement equations in expanded forms are summarized as follows

$$\sigma_{xx}^{P} = C_{11}(\varepsilon_{xx} - \alpha_{xx}^{P}(T)\Delta T) + C_{12}(\varepsilon_{\theta\theta} - \alpha_{\theta\theta}^{P}(T)\Delta T) - e_{31}E_x, \tag{19}$$

$$\sigma_{\theta\theta}^{P} = C_{12}(\varepsilon_{xx} - \alpha_{xx}^{P}(T)\Delta T) + C_{11}(\varepsilon_{\theta\theta} - \alpha_{\theta\theta}^{P}(T)\Delta T) - e_{31}E_x, \tag{20}$$

$$\sigma_{\theta z}^{P} = C_{44}\gamma_{\theta z}, \tag{21}$$

$$\sigma_{xx}^{P} = C_{55}\gamma_{zx}, \tag{22}$$

$$\sigma_{x\theta}^{P} = C_{66}\gamma_{x\theta}, \tag{23}$$

$$D_{xx} = e_{31}\varepsilon_{xx} + e_{31}\varepsilon_{\theta\theta} + K_{11}E_x. \tag{24}$$

3.3 Deriving motion equations

In this investigation, energy method has been used to derive higher order motion equations. Its familiar form can be written as

$$\int_0^T \left(\delta U_{tot} - \delta W_{tot} - \delta K_{tot}\right)dt = 0, \tag{25}$$

where U_{tot}, K_{tot} and W_{tot} are total potential energy, total kinetic energy and work done by external forces, respectively.

3.3.1 Potential energy

The virtual potential energy of piezoelectric layer can be expressed as

$$\delta U_P = \int_S \int_0^{hp} \left(\sigma_{xx}^{P}\delta\varepsilon_{xx} + \sigma_{\theta\theta}^{P}\delta\varepsilon_{\theta\theta} + \sigma_{x\theta}^{P}\delta\gamma_{x\theta} + \sigma_{\theta z}^{P}\delta\gamma_{\theta z} + \sigma_{zx}^{P}\delta\gamma_{zx} - D_{xx}\,\delta E_x\right)dz\,dA. \tag{26}$$

On the other hand, the virtual potential energy of CNTRC cylindrical shell can be written as

$$\delta U_s = \frac{1}{2}\int_{\Omega_0}\int_{-h/2}^{h/2}\left(\sigma_{xx}\delta\varepsilon_{xx} + \sigma_{\theta\theta}\delta\varepsilon_{\theta\theta} + \sigma_{x\theta}\delta\gamma_{x\theta} + \sigma_{xz}\delta\gamma_{xz} + \sigma_{\theta z}\delta\gamma_{\theta z}\right)dV \tag{27}$$

However, the total virtual potential energy of system is obtained as follows

$$\begin{aligned}\delta U_{tot} = \delta U_s + \delta U_P = \int_S \{ \int \big[&\left(\sigma_{xx} + \sigma_{xx}^{P}\right)\left(\delta\varepsilon_{xx}^{0} + z\delta\varepsilon_{xx}^{1}\right) + \left(\sigma_{\theta\theta} + \sigma_{\theta\theta}^{P}\right)\left(\delta\varepsilon_{\theta\theta}^{0} + z\delta\varepsilon_{\theta\theta}^{1}\right)\\ &+ \left(\sigma_{x\theta} + \sigma_{x\theta}^{P}\right)\left(\delta\gamma_{x\theta}^{0} + z\delta\gamma_{x\theta}^{1}\right) + \left(\sigma_{z\theta} + \sigma_{z\theta}^{P}\right)\left(\delta\gamma_{z\theta}^{0} + z\delta\gamma_{z\theta}^{1}\right)\\ &+ \left(\sigma_{xz} + \sigma_{xz}^{P}\right)\left(\delta\gamma_{xz}^{0} + z\delta\gamma_{xz}^{1}\right) - D_{xx}\delta E_x\big]dz\}dA.\end{aligned} \tag{28}$$

Now, substituting Eq. (14) and into Eq. (28) and simplifying the statements, the following integration equation is obtained

$$\delta U_{tot} = \int_S [N_{xx}\delta\varepsilon^0_{xx} + M_{xx}\delta\varepsilon^1_{xx} + N_{\theta\theta}\delta\varepsilon^0_{\theta\theta} + M_{\theta\theta}\delta\varepsilon^1_{\theta\nu} + N_{x\theta}\delta\gamma^0_{x\theta} + M_{x\theta}\delta\gamma^1_{x\theta} + Q_x\delta\gamma^0_{xz} + Q_\theta\delta\gamma^0_{\theta z} - G_{xx}\delta E_x]dA \tag{29}$$

where stress and moment resultants can be calculated as

$$\begin{bmatrix} N_{xx} \\ N_{\theta\theta} \\ N_{x\theta} \\ G_{xx} \end{bmatrix} = \int_{-h-h_P}^{-h} \begin{bmatrix} \sigma^P_{xx} \\ \sigma^P_{\theta\theta} \\ \sigma^P_{x\theta} \\ D_{xx} \end{bmatrix} dz + \int_{-h}^{h} \begin{bmatrix} \sigma_{xx} \\ \sigma_{\theta\theta} \\ \sigma_{x\theta} \\ 0 \end{bmatrix} dz + \int_{h}^{h+h_P} \begin{bmatrix} \sigma^P_{xx} \\ \sigma^P_{\theta\theta} \\ \sigma^P_{x\theta} \\ D_{xx} \end{bmatrix} dz \tag{30}$$

$$\begin{bmatrix} M_{xx} \\ M_{\theta\theta} \\ M_{x\theta} \end{bmatrix} = \int_{-h-h_P}^{-h} \begin{bmatrix} \sigma^P_{xx} \\ \sigma^P_{\theta\theta} \\ \sigma^P_{x\theta} \end{bmatrix} zdz + \int_{-h}^{h} \begin{bmatrix} \sigma_{xx} \\ \sigma_{\theta\theta} \\ \sigma_{x\theta} \end{bmatrix} zdz + \int_{h}^{h+h_P} \begin{bmatrix} \sigma^P_{xx} \\ \sigma^P_{\theta\theta} \\ \sigma^P_{x\theta} \end{bmatrix} zdz \tag{31}$$

$$\begin{bmatrix} Q_x \\ Q_\theta \end{bmatrix} = k' \int_{-h-h_P}^{-h} \begin{bmatrix} \sigma^P_{xz} \\ \sigma^P_{\theta z} \end{bmatrix} dz + k' \int_{-h}^{h} \begin{bmatrix} \sigma_{xz} \\ \sigma_{\theta z} \end{bmatrix} zdz + k' \int_{h}^{h+h_P} \begin{bmatrix} \sigma^P_{xz} \\ \sigma^P_{\theta z} \end{bmatrix} zdz \tag{32}$$

In which k' is shear correction coefficient.

3.3.2 Kinetic energy

The virtual kinetic energy of piezoelectric layer may be written as

$$K = \int_S \left(\int \rho_P \left(\dot{u}\delta\dot{u} + \dot{v}\delta\dot{v} + \dot{w}\delta\dot{w} \right) dz \right) dA \tag{33}$$

On the other hand, the virtual kinetic energy of CNTRC cylindrical shell can be written as

$$K = \int_S \left(\int \rho_s(z) \left(\dot{u}\delta\dot{u} + \dot{v}\delta\dot{v} + \dot{w}\delta\dot{w} \right) dz \right) dA \tag{34}$$

where ρ_s and ρ_P are density of CNTRC cylindrical shell and piezoelectric layers, respectively. Now, substituting Eq. (13) into Eq. (34) and simplifying the statements, the following integration equation is obtained

$$\delta K_{tot} = \int_S [I_0(\dot{u}\delta\dot{u} + \dot{v}\delta\dot{v} + \dot{w}\delta\dot{w}) + I_1(\dot{u}\delta\dot{\psi}_x + \dot{\psi}_x\delta\dot{u} + \dot{v}\delta\dot{\psi}_\theta + \dot{\psi}_\theta\delta\dot{v}) + I_2(\dot{\psi}_x\delta\dot{\psi}_x + \dot{\psi}_\theta\delta\dot{\psi}_\theta)]dA, \tag{35}$$

where the mass moment of inertia may be written as

$$\begin{bmatrix} I_0 \\ I_1 \\ I_2 \end{bmatrix} = \int_{-h-h_P}^{-h} \begin{bmatrix} \rho_P \\ \rho_P z \\ \rho_P z^2 \end{bmatrix} dz + \int_{-h}^{h} \begin{bmatrix} \rho_s(z) \\ \rho_s(z) z \\ \rho_s(z) z^2 \end{bmatrix} dz + \int_{h}^{h+h_P} \begin{bmatrix} \rho_P \\ \rho_P z \\ \rho_P z^2 \end{bmatrix} dz \tag{36}$$

3.3.3 Work done

In this paper, the work done is due to elastic medium and viscous fluid which can be written as

$$W = \int_0^L \left(P_{Fluid} + P_{Elastic}\right) w dx, \tag{37}$$

❖ *Viscous fluid work*

Consider the flow of fluid in inner layer of system in which the flow is assumed to be axially symmetric, Newtonian, laminar and fully developed. The basic momentum governing equation of the flow simplifies to

$$\rho_b \frac{\partial v_r}{\partial t} = -\frac{\partial P}{\partial r} + \frac{1}{r}\frac{\partial \tau_{r\theta}}{\partial \theta} - \frac{\tau_{\theta\theta}}{r} + \frac{\partial \tau_{xr}}{\partial x}, \tag{38}$$

where ρ_b and $P$are fluid mass density and flow fluid pressure, respectively. The fluid force acted on the system can be calculated from Eq. (38). Since the velocity and acceleration of the cylindrical shell and fluid at the point of contact between them are equal (Wang and Ni 2009), the fluid flow work may be written as

$$\begin{aligned} q_{Fluid} = \Bigg[& -\rho_f h_f \left(\frac{\partial^2 w}{\partial t^2} + 2v_x \frac{\partial^2 w}{\partial x \partial t} + v_x^2 \frac{\partial^2 w}{\partial x^2} \right) + \frac{h_f}{R^2} \frac{\partial}{\partial \theta} \left(\mu \left(\frac{\partial^2 w}{\partial \theta \partial t} + v_x \frac{\partial^2 w}{\partial \theta \partial x} \right) \right) \\ & - \frac{2h_f}{R} \left(\mu \left(\frac{\partial w}{\partial t} + v_x \frac{\partial w}{\partial x} \right) \right) + h_f \frac{\partial}{\partial x} \left(\mu \left(\frac{\partial^2 w}{\partial x \partial t} + v_x \frac{\partial^2 w}{\partial x^2} \right) \right) \Bigg], \end{aligned} \tag{39}$$

where ρ_f is density of fluid.

❖ *Orthotropic Pasternak foundation*

The external force of orthotropic Pasternak medium can be expressed as (Kutlu and Omurtag 2012, Benrahou *et al*. 2015)

$$\begin{aligned} P = {} & K_W w - K_{g\xi} \left(\cos^2\theta \frac{\partial^2 w}{\partial x^2} + 2\cos\theta \sin\theta \frac{\partial^2 w}{R \partial x \partial \theta} + \sin^2\theta \frac{\partial^2 w}{R^2 \partial \theta^2} \right) \\ & - K_{g\eta} \left(\sin^2\theta \frac{\partial^2 w}{\partial x^2} - 2\sin\theta \cos\theta \frac{\partial^2 w}{R \partial x \partial \theta} + \cos^2\theta \frac{\partial^2 w}{R^2 \partial \theta^2} \right), \end{aligned} \tag{40}$$

where angle θ describes the local ξ direction of orthotropic foundation with respect to the global x-axis of the shell. Since the surrounding medium is relatively soft, the foundation stiffness K_W may be expressed by

$$K_W = \frac{E_0}{4L(1-\nu_0^2)(2-c_1)^2}\left[5-\left(2\gamma_1^2+6\gamma_1+5\right)\exp\left(-2\gamma_1\right)\right], \tag{41}$$

where

$$c_1 = \left(\gamma_1+2\right)\exp\left(-\gamma_1\right), \tag{42}$$

$$\gamma_1 = \frac{H_s}{L}, \tag{43}$$

$$E_0 = \frac{E_s}{(1-\nu_s^2)}, \tag{44}$$

$$\nu_0 = \frac{\nu_s}{(1-\nu_s)}, \tag{45}$$

where E_s, ν_s, H_s are Young's modulus, Poisson's ratio and depth of the foundation, respectively. In this paper, E_s is assumed to be temperature-dependent while ν_s is assumed to be a constant.

Finally, substituting Eqs. (29), (35) and (37) into Eq. (29) yields the following governing equations

$$\delta u : \frac{\partial N_{xx}}{\partial x}+\frac{\partial N_{x\theta}}{R\partial\theta} = I_0\frac{\partial^2 u}{\partial t^2}+I_1\frac{\partial^2 \psi_x}{\partial t^2}, \tag{46}$$

$$\delta v : \frac{\partial N_{x\theta}}{\partial x}+\frac{\partial N_{\theta\theta}}{R\partial\theta}+\frac{Q_\theta}{R} = I_0\frac{\partial^2 v}{\partial t^2}+I_1\frac{\partial^2 \psi_\theta}{\partial t^2}, \tag{47}$$

$$\delta w : \frac{\partial Q_x}{\partial x}+\frac{\partial Q_\theta}{R\partial\theta}-\frac{N_{\theta\theta}}{R}+\frac{\partial}{\partial x}\left(N_{xx}\frac{\partial w}{\partial x}+N_{x\theta}\frac{\partial w}{R\partial\theta}\right)+\frac{\partial}{R\partial\theta}\left(N_{x\theta}\frac{\partial w}{\partial x}+N_{\theta\theta}\frac{\partial w}{R\partial\theta}\right)+P = I_0\frac{\partial^2 w}{\partial t^2}, \tag{48}$$

$$\delta\psi_x : \frac{\partial M_{xx}}{\partial x}+\frac{\partial M_{x\theta}}{R\partial\theta}-Q_x = I_2\frac{\partial^2 \psi_x}{\partial t^2}+I_1\frac{\partial^2 u}{\partial t^2}, \tag{49}$$

$$\delta\psi_\theta : \frac{\partial M_{x\theta}}{\partial x}+\frac{\partial M_{\theta\theta}}{R\partial\theta}-Q_\theta = I_2\frac{\partial^2 \psi_\theta}{\partial t^2}+I_1\frac{\partial^2 v}{\partial t^2}, \tag{50}$$

$$\delta\phi : \frac{\partial G_{xx}}{\partial x} = 0, \tag{51}$$

where in above relations, substituting Eqs. (15) and (19)-(24) into Eqs. (30)-(32), the stress resultant-displacement relations can be obtained as follow

$$
\begin{aligned}
N_{xx} &= A_{110}\left(\frac{\partial u}{\partial x}+\frac{1}{2}\left(\frac{\partial w}{\partial x}\right)^2\right)+A_{111}\left(\frac{\partial \psi_x}{\partial x}\right)+A_{120}\left(\frac{\partial v}{R\partial\theta}+\frac{w}{R}+\frac{1}{2}\left(\frac{\partial w}{R\partial\theta}\right)^2\right)+A_{121}\left(\frac{\partial \psi_\theta}{R\partial\theta}\right)-N_{xx}^T,\\
N_{\theta\theta} &= A_{120}\left(\frac{\partial u}{\partial x}+\frac{1}{2}\left(\frac{\partial w}{\partial x}\right)^2\right)+A_{121}\left(\frac{\partial \psi_x}{\partial x}\right)+A_{220}\left(\frac{\partial v}{R\partial\theta}+\frac{w}{R}+\frac{1}{2}\left(\frac{\partial w}{R\partial\theta}\right)^2\right)+A_{221}\left(\frac{\partial \psi_\theta}{R\partial\theta}\right)-N_{\theta\theta}^T,\\
N_{x\theta} &= A_{660}\left(\frac{\partial u}{R\partial\theta}+\frac{\partial v}{\partial x}+\frac{\partial w}{\partial x}\frac{\partial w}{R\partial\theta}\right)+A_{661}\left(\frac{\partial \psi_x}{R\partial\theta}+\frac{\partial \psi_\theta}{\partial x}\right),
\end{aligned}
\tag{52}
$$

$$
\begin{aligned}
M_{xx} &= A_{111}\left(\frac{\partial u}{\partial x}+\frac{1}{2}\left(\frac{\partial w}{\partial x}\right)^2\right)+A_{112}\left(\frac{\partial \psi_x}{\partial x}\right)+A_{121}\left(\frac{\partial v}{R\partial\theta}+\frac{w}{R}+\frac{1}{2}\left(\frac{\partial w}{R\partial\theta}\right)^2\right)+A_{122}\left(\frac{\partial \psi_\theta}{R\partial\theta}\right)-M_{xx}^T,\\
M_{\theta\theta} &= A_{121}\left(\frac{\partial u}{\partial x}+\frac{1}{2}\left(\frac{\partial w}{\partial x}\right)^2\right)+A_{122}\left(\frac{\partial \psi_x}{\partial x}\right)+A_{221}\left(\frac{\partial v}{R\partial\theta}+\frac{w}{R}+\frac{1}{2}\left(\frac{\partial w}{R\partial\theta}\right)^2\right)+A_{222}\left(\frac{\partial \psi_\theta}{R\partial\theta}\right)-M_{\theta\theta}^T,\\
M_{x\theta} &= A_{661}\left(\frac{\partial u}{R\partial\theta}+\frac{\partial v}{\partial x}+\frac{\partial w}{\partial x}\frac{\partial w}{R\partial\theta}\right)+A_{662}\left(\frac{\partial \psi_x}{R\partial\theta}+\frac{\partial \psi_\theta}{\partial x}\right),
\end{aligned}
\tag{53}
$$

$$
\begin{aligned}
Q_x &= k'A_{55}\left(\frac{\partial w}{\partial x}+\psi_x\right),\\
Q_\theta &= k'A_{44}\left(\frac{\partial w}{R\partial\theta}-\frac{v}{R}+\psi_\theta\right),
\end{aligned}
\tag{54}
$$

$$
G_{xx} = 2e_{31}h_p\left(\frac{\partial u}{\partial x}+\frac{1}{2}\left(\frac{\partial w}{\partial x}\right)^2\right)+2e_{31}h_p\left(\frac{\partial v}{R\partial\theta}+\frac{w}{R}+\frac{1}{2}\left(\frac{\partial w}{R\partial\theta}\right)^2\right)-2K_{11}h_p\left(\frac{\partial \phi}{\partial x}\right),
\tag{55}
$$

where

$$
A_{11k} = \int_{-h-h_P}^{-h} C_{11}z^k dz + \int_{-h}^{h} Q_{11}(z)z^k dz + \int_{h}^{h+h_P} C_{11}z^k dz, \qquad k = 0,1,2
\tag{56}
$$

$$
A_{12k} = \int_{-h-h_P}^{-h} C_{12}z^k dz + \int_{-h}^{h} Q_{12}(z)z^k dz + \int_{h}^{h+h_P} C_{12}z^k dz, \qquad k = 0,1,2
\tag{57}
$$

$$
A_{22k} = \int_{-h-h_P}^{-h} C_{22}z^k dz + \int_{-h}^{h} Q_{22}(z)z^k dz + \int_{h}^{h+h_P} C_{22}z^k dz, \qquad k = 0,1,2
\tag{58}
$$

$$
A_{66k} = \int_{-h-h_P}^{-h} C_{66}z^k dz + \int_{-h}^{h} Q_{66}(z)z^k dz + \int_{h}^{h+h_P} C_{66}z^k dz, \qquad k = 0,1,2
\tag{59}
$$

$$A_{44} = \int_{-h-h_P}^{-h} C_{44} dz + \int_{-h}^{h} Q_{44}(z) dz + \int_{h}^{h+h_P} C_{44} dz, \tag{60}$$

$$A_{55} = \int_{-h-h_P}^{-h} C_{55} z^k dz + \int_{-h}^{h} Q_{55}(z) z^k dz + \int_{h}^{h+h_P} C_{55} z^k dz. \tag{61}$$

Furthermore, (N_{xx}^T, N_{yy}^T) and (M_{xx}^T, M_{yy}^T) are thermal force and thermal moment resultants, respectively, and are given by

$$\begin{Bmatrix} N_{xx}^T \\ N_{\theta\theta}^T \end{Bmatrix} = \int_{-h-h_P}^{-h} \begin{Bmatrix} C_{11}(T)\alpha_{xx}^P + C_{12}(T)\alpha_{\theta\theta}^P \\ C_{21}(T)\alpha_{xx}^P + C_{22}(T)\alpha_{\theta\theta}^P \end{Bmatrix} \Delta T\, dz + \int_{-h}^{h} \begin{Bmatrix} Q_{11}(z,T)\alpha_{xx} + Q_{12}(z,T)\alpha_{\theta\theta} \\ Q_{21}(z,T)\alpha_{xx} + Q_{22}(z,T)\alpha_{\theta\theta} \end{Bmatrix} \Delta T\, dz + \int_{h}^{h+h_P} \begin{Bmatrix} C_{11}(T)\alpha_{xx}^P + C_{12}(T)\alpha_{\theta\theta}^P \\ C_{21}(T)\alpha_{xx}^P + C_{22}(T)\alpha_{\theta\theta}^P \end{Bmatrix} \Delta T\, dz, \tag{62}$$

$$\begin{Bmatrix} M_{xx}^T \\ M_{\theta\theta}^T \end{Bmatrix} = \int_{-h-h_P}^{-h} \begin{Bmatrix} C_{11}(T)\alpha_{xx}^P + C_{12}(T)\alpha_{\theta\theta}^P \\ C_{21}(T)\alpha_{xx}^P + C_{22}(T)\alpha_{\theta\theta}^P \end{Bmatrix} \Delta T\, z dz + \int_{-h}^{h} \begin{Bmatrix} Q_{11}(z,T)\alpha_{xx} + Q_{12}(z,T)\alpha_{\theta\theta} \\ Q_{21}(z,T)\alpha_{xx} + Q_{22}(z,T)\alpha_{\theta\theta} \end{Bmatrix} \Delta T\, z dz + \int_{h}^{h+h_P} \begin{Bmatrix} C_{11}(T)\alpha_{xx}^P + C_{12}(T)\alpha_{\theta\theta}^P \\ C_{21}(T)\alpha_{xx}^P + C_{22}(T)\alpha_{\theta\theta}^P \end{Bmatrix} \Delta T\, z dz, \tag{63}$$

Substituting Eqs. (52) to (63) into Eqs. (46) to (51), the governing equations can be written as follow

δu:

$$\frac{\partial}{\partial x}\left(A_{110}\left(\frac{\partial u}{\partial x} + \frac{1}{2}\left(\frac{\partial w}{\partial x} \right)^2 \right) + A_{111}\left(\frac{\partial \psi_x}{\partial x} \right) + A_{120}\left(\frac{\partial v}{R\partial\theta} + \frac{w}{R} + \frac{1}{2}\left(\frac{\partial w}{R\partial\theta} \right)^2 \right) + A_{121}\left(\frac{\partial \psi_\theta}{R\partial\theta} \right) \right)$$
$$\frac{\partial}{R\partial\theta}\left(A_{660}\left(\frac{\partial u}{R\partial\theta} + \frac{\partial v}{\partial x} + \frac{\partial w}{\partial x}\frac{\partial w}{R\partial\theta} \right) + A_{661}\left(\frac{\partial \psi_x}{R\partial\theta} + \frac{\partial \psi_\theta}{\partial x} \right) \right) = I_0 \frac{\partial^2 u}{\partial t^2} + I_1 \frac{\partial^2 \psi_x}{\partial t^2}, \tag{64}$$

δv:

$$\frac{\partial}{R\partial\theta}\left(A_{120}\left(\frac{\partial u}{\partial x} + \frac{1}{2}\left(\frac{\partial w}{\partial x} \right)^2 \right) + A_{121}\left(\frac{\partial \psi_x}{\partial x} \right) + A_{220}\left(\frac{\partial v}{R\partial\theta} + \frac{w}{R} + \frac{1}{2}\left(\frac{\partial w}{R\partial\theta} \right)^2 \right) + A_{221}\left(\frac{\partial \psi_\theta}{R\partial\theta} \right) \right)$$
$$+ \frac{\partial}{\partial x}\left(A_{660}\left(\frac{\partial u}{R\partial\theta} + \frac{\partial v}{\partial x} + \frac{\partial w}{\partial x}\frac{\partial w}{R\partial\theta} \right) + A_{661}\left(\frac{\partial \psi_x}{R\partial\theta} + \frac{\partial \psi_\theta}{\partial x} \right) \right)$$
$$+ \frac{1}{R}\left(k' A_{44}\left(\frac{\partial w}{R\partial\theta} - \frac{v}{R} + \psi_\theta \right) \right) = I_0 \frac{\partial^2 v}{\partial t^2} + I_1 \frac{\partial^2 \psi_\theta}{\partial t^2}, \tag{65}$$

δw:

$$\frac{\partial}{\partial x}\left(k'A_{55}\left(\frac{\partial w}{\partial x}+\psi_x\right)\right)+\frac{\partial}{R\partial\theta}\left(k'A_{44}\left(\frac{\partial w}{R\partial\theta}-\frac{v}{R}+\psi_\theta\right)\right)-\frac{1}{R}\left(A_{120}\left(\frac{\partial u}{\partial x}+\frac{1}{2}\left(\frac{\partial w}{\partial x}\right)^2\right)+A_{121}\left(\frac{\partial\psi_x}{\partial x}\right)\right.$$
$$\left.+A_{220}\left(\frac{\partial v}{R\partial\theta}+\frac{w}{R}+\frac{1}{2}\left(\frac{\partial w}{R\partial\theta}\right)^2\right)+A_{221}\left(\frac{\partial\psi_\theta}{R\partial\theta}\right)\right)+\left(N_{xx}^T+N_{xx}^M\right)\frac{\partial^2 w}{\partial x^2}+\left(N_{\theta\theta}^T+N_{\theta\theta}^M\right)\frac{\partial^2 w}{R^2\partial\theta^2} \tag{66}$$
$$+\left[-\rho_f h_f\left(\frac{\partial^2 w}{\partial t^2}+2v_x\frac{\partial^2 w}{\partial x\partial t}+v_x^2\frac{\partial^2 w}{\partial x^2}\right)+\frac{h_f}{R^2}\frac{\partial}{\partial\theta}\left(\mu\left(\frac{\partial^2 w}{\partial\theta\partial t}+v_x\frac{\partial^2 w}{\partial\theta\partial x}\right)\right)\right.$$
$$\left.-\frac{2h_f}{R}\left(\mu\left(\frac{\partial w}{\partial t}+v_x\frac{\partial w}{\partial x}\right)\right)+h_f\frac{\partial}{\partial x}\left(\mu\left(\frac{\partial^2 w}{\partial x\partial t}+v_x\frac{\partial^2 w}{\partial x^2}\right)\right)\right]+K_W w$$
$$-K_{g\xi}\left(\cos^2\theta\frac{\partial^2 w}{\partial x^2}+2\cos\theta\sin\theta\frac{\partial^2 w}{R\partial x\partial\theta}+\sin^2\theta\frac{\partial^2 w}{R^2\partial\theta^2}\right)$$
$$-K_{g\eta}\left(\sin^2\theta\frac{\partial^2 w}{\partial x^2}-2\sin\theta\cos\theta\frac{\partial^2 w}{R\partial x\partial\theta}+\cos^2\theta\frac{\partial^2 w}{R^2\partial\theta^2}\right)=I_0\frac{\partial^2 w}{\partial t^2},$$

(66)

$\delta\psi_x$:

$$\frac{\partial}{\partial x}\left(A_{111}\left(\frac{\partial u}{\partial x}+\frac{1}{2}\left(\frac{\partial w}{\partial x}\right)^2\right)+A_{112}\left(\frac{\partial\psi_x}{\partial x}\right)+A_{121}\left(\frac{\partial v}{R\partial\theta}+\frac{w}{R}+\frac{1}{2}\left(\frac{\partial w}{R\partial\theta}\right)^2\right)+A_{122}\left(\frac{\partial\psi_\theta}{R\partial\theta}\right)\right)$$
$$+\frac{\partial}{R\partial\theta}\left(A_{661}\left(\frac{\partial u}{R\partial\theta}+\frac{\partial v}{\partial x}+\frac{\partial w}{\partial x}\frac{\partial w}{R\partial\theta}\right)+A_{662}\left(\frac{\partial\psi_x}{R\partial\theta}+\frac{\partial\psi_\theta}{\partial x}\right)\right) \tag{67}$$
$$-k'A_{55}\left(\frac{\partial w}{\partial x}+\psi_x\right)=I_2\frac{\partial^2\psi_x}{\partial t^2}+I_1\frac{\partial^2 u}{\partial t^2},$$

$\delta\psi_\theta$:

$$\frac{\partial}{R\partial\theta}\left(A_{121}\left(\frac{\partial u}{\partial x}+\frac{1}{2}\left(\frac{\partial w}{\partial x}\right)^2\right)+A_{122}\left(\frac{\partial\psi_x}{\partial x}\right)+A_{221}\left(\frac{\partial v}{R\partial\theta}+\frac{w}{R}+\frac{1}{2}\left(\frac{\partial w}{R\partial\theta}\right)^2\right)+A_{222}\left(\frac{\partial\psi_\theta}{R\partial\theta}\right)\right)$$
$$+\frac{\partial}{\partial x}\left(A_{661}\left(\frac{\partial u}{R\partial\theta}+\frac{\partial v}{\partial x}+\frac{\partial w}{\partial x}\frac{\partial w}{R\partial\theta}\right)+A_{662}\left(\frac{\partial\psi_x}{R\partial\theta}+\frac{\partial\psi_\theta}{\partial x}\right)\right) \tag{68}$$
$$-k'A_{44}\left(\frac{\partial w}{R\partial\theta}-\frac{v}{R}+\psi_\theta\right)=I_2\frac{\partial^2\psi_\theta}{\partial t^2}+I_1\frac{\partial^2 v}{\partial t^2},$$

$\delta\phi$:

$$\frac{\partial}{\partial x}\left(2e_{31}h_p\left(\frac{\partial u}{\partial x}+\frac{1}{2}\left(\frac{\partial w}{\partial x}\right)^2\right)+2e_{31}h_p\left(\frac{\partial v}{R\partial\theta}+\frac{w}{R}+\frac{1}{2}\left(\frac{\partial w}{R\partial\theta}\right)^2\right)-2K_{11}h_p\left(\frac{\partial\phi}{\partial x}\right)\right)=0. \tag{69}$$

4. DQM

In this method, the differential equations are changed into a first order algebraic equation by employing appropriate weighting coefficients. Because weighting coefficients do not relate to any special problem and only depend on the grid spacing. In other words, the partial derivatives of a function (say w here) are approximated with respect to specific variables (say x and θ), at a discontinuous point in a defined domain as a set of linear weighting coefficients and the amount represented by the function itself at that point and other points throughout the domain. The approximation of the n^{th} and m^{th} derivatives function with respect to x and y, respectively may be expressed in general form as (Ghorbanpour Arani *et al*. 2013).

$$\begin{aligned} f_x{}^{(n)}(x_i,\theta_i)&=\sum_{k=1}^{N_x}A^{(n)}{}_{ik}f(x_k,\theta_j),\\ f_\theta{}^{(m)}(x_i,\theta_i)&=\sum_{l=1}^{N_\theta}B^{(m)}{}_{jl}f(x_i,\theta_l),\\ f_{x\theta}{}^{(n+m)}(x_i,\theta_i)&=\sum_{k=1}^{N_x}\sum_{l=1}^{N_\theta}A^{(n)}{}_{ik}B^{(m)}{}_{jl}f(x_k,\theta_l), \end{aligned} \tag{70}$$

where N_x and N_θ, denotes the number of points in x and θ directions, $f(x, \theta)$ is the function and A_{jk}, B_{jl} are the weighting coefficients (Ghorbanpour Arani *et al*. 2013). The solution of the motion equations can be assumed as follows

$$d(x,\theta,t)=d_0(x,\theta)e^{\omega\tau},\quad d_0=u_0,v_0,w_0,\psi_{x0},\psi_{\theta0},\phi_0 \tag{71}$$

where $\omega=\lambda h\sqrt{\frac{\rho_f}{E}}$ is the dimensionless natural frequency and λ is the (Fundamental) natural frequency. Finally, the governing equations in matrix form can be expressed as

$$\left[[K_L+K_{NL}]+[C]\omega+[M]\omega^2\right][d_0]=[0], \tag{72}$$

where [*KL*] and [*KNL*] are respectively, linear and nonlinear stiffness matrixes; [*C*] is damp matrix and [*M*] is the mass matrix. For solving the Eq. (72) and reducing it to the standard form of eigenvalue problem, it is convenient to rewrite Eq. (72) as the following first order variable as

$$\{\dot{Z}\} = [A]\{Z\}, \tag{73}$$

in which the state vector Z and state matrix $[A]$ are defined as

$$Z = \begin{Bmatrix} d_d \\ \dot{d}_d \end{Bmatrix} \text{ and } [A] = \begin{bmatrix} [0] & [I] \\ -[M^{-1}(K_L + K_{NL})] & -[M^{-1}C] \end{bmatrix}, \tag{74}$$

where [0] and [I] are the zero and unitary matrices, respectively. However, the frequencies obtained from the solution of Eq. (72) are complex due to the damping existed in the presence of the viscous fluid flow. Hence, the results are containing two real and imaginary parts. The real part is corresponding to the system damping, and the imaginary part representing the system natural frequencies.

5. Numerical results

This section reports the outcome of nonlinear analyses and instability of simply supported (Najafov *et al*. 2014) piezoelectric sandwich cylindrical shell for comparison and verification of accuracy as well as effectiveness of the present method. Then detailed parametric studies are presented to illustrate the nonlinear responses of CNTRC cylindrical shell integrated with piezoelectric layers. Poly{(m-phenylenevinylene)-co-[(2,5-dioctoxy-pphenylene) vinylene]}, referred as PmPV, is selected as the matrix with isotropic material properties v_m = 0.34 and E_m = (3.51 – 0.0047T) GPa, where $T = T_0 + \Delta T$ and $T_0 = 300$ K (room temperature). As material properties of SWCNTs are charity, size and temperature-dependent, typical values are taken from analytical results of Shen (2009). Furthermore, the piezoelectric layers are made from PZT-5A with elastic and thermal constants of E = 61(1 – 0.005ΔT) GPa and α = 0.9 × 10^{-6} (1 + 0.0005ΔT) 1/K. The elastomeric medium is made of Poly dimethylsiloxane (PDMS) which the temperature-dependent material properties of which are assumed to be v_s = 0.48 and E_s = (3.22 – 0.0034T) GPa in which T = T_0 + ΔT and T_0 = 300 K (room temperature) (Shen 2009). For the present analysis, fourteen DQ grid points is used which yields accurate results.

Figs. 2(a) and (b) show the effect of distribution type of SWCNT in cylindrical shell on the dimensionless natural frequency (Im(ω) and damping (Re(ω)) of sandwich structure versus dimensionless flow velocity ($U = \sqrt{\rho_f / C_{11}}\, v_x$), respectively. For the CNTRC cylindrical shell, UD and three types of FG distribution patterns of SWCNT reinforcements are assumed. As can be seen, Im(ω) decreases with increasing U, while the Re(ω) remains zero. These imply that the system is stable. When the natural frequency becomes zero, critical velocity is reached, which the system loses its stability due to the divergence via a pitchfork bifurcation. Hence, the eigen frequencies have the positive real parts, which the system becomes unstable. In this state, both real and imaginary parts of frequency become zero at the same point. It is worth to note that for these four types of CNTRC cylindrical shell that have the same mass fraction of CNTs, FGO cylindrical shell have the lowest values of the non-dimensional frequency and the maximum values of the non-dimensional frequency occurs for FGX cylindrical shell. We can conclude that CNTs

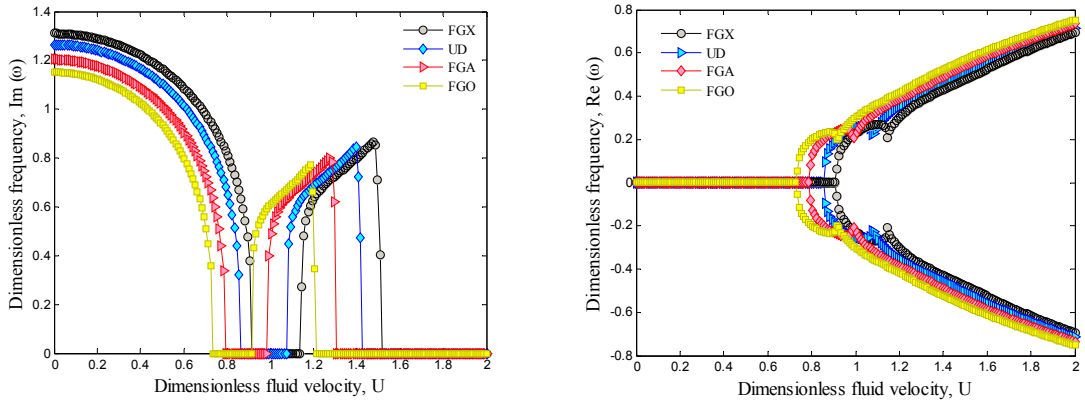

(a) (b)

Fig. 2 Effects of CNT distribution on the (a) dimension frequency (Im(ω)); (b) dimension frequency (Re(ω)) versus dimension flow velocity

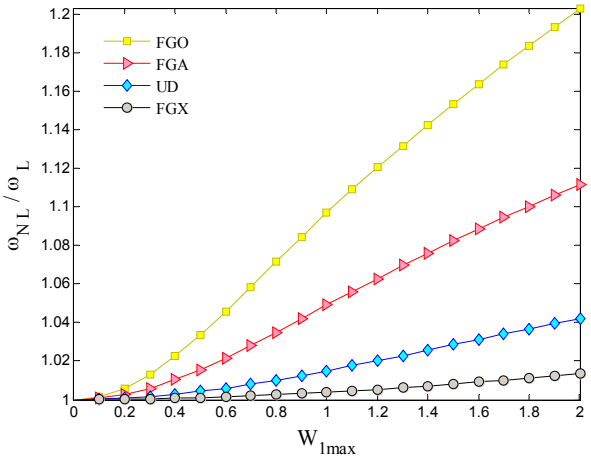

Fig. 3 Effects of CNT distribution on frequency ration versus maximum amplitude

distributed close to top and bottom surfaces are more efficient in increasing the stiffness of the cylindrical shell than CNTs distributed near the mid-plane. Therefore, designers can obtain desired stiffness of CNTRC cylindrical shell by regulating distributions of CNTs.

Fig. 3 illustrates the nonlinear to linear frequency of sandwich structure with respect to maximum amplitude for different types of FG-CNTRC cylindrical shell. It can be concluded that the FGX and FGO patterns have minimum and maximum frequency ratio, respectively. Furthermore, with increasing maximum amplitude, the effect of CNT patterns on frequency ration of sandwich structure becomes more considerable.

Effects of the SWCNT volume fraction on the dimensionless natural frequency and damping of the system are presented in Figs. 4(a) and (b). It can be observed that the frequency and critical fluid velocity of the system increases with increasing volume fraction of CNTs since stiffness of sandwich structure increases when the CNT volume increases.

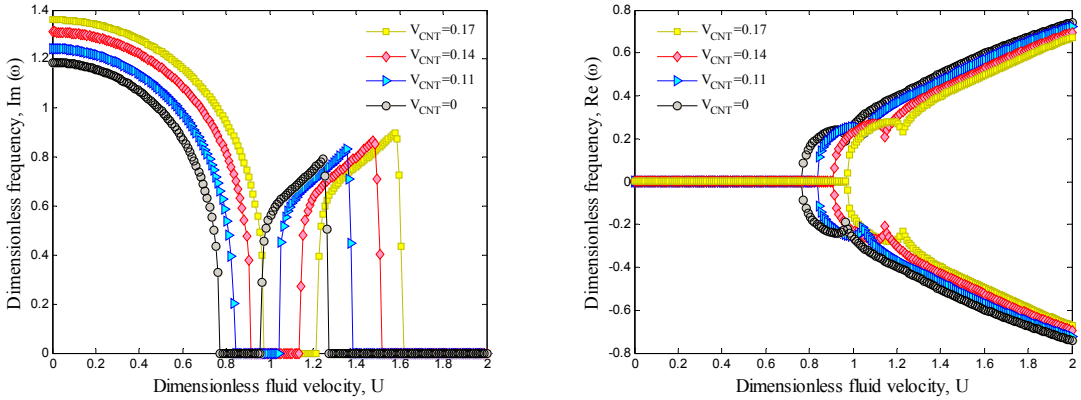

(a) (b)

Fig. 4 Effects of CNT volume fraction on the (a) dimension frequency (Im(ω)); (b) dimension frequency (Re(ω)) versus dimension flow velocity

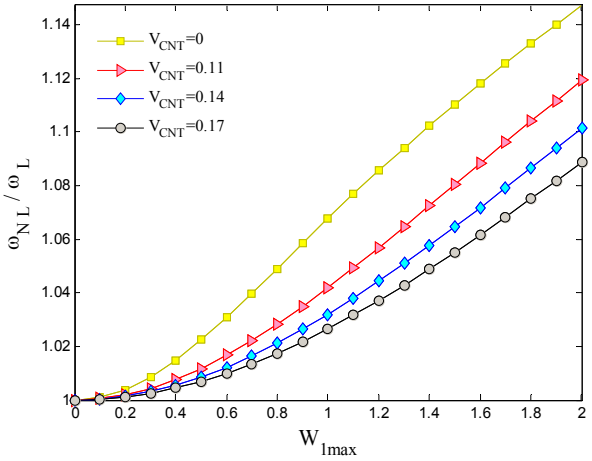

Fig. 5 Effects of CNT volume fraction on frequency ration versus maximum amplitude

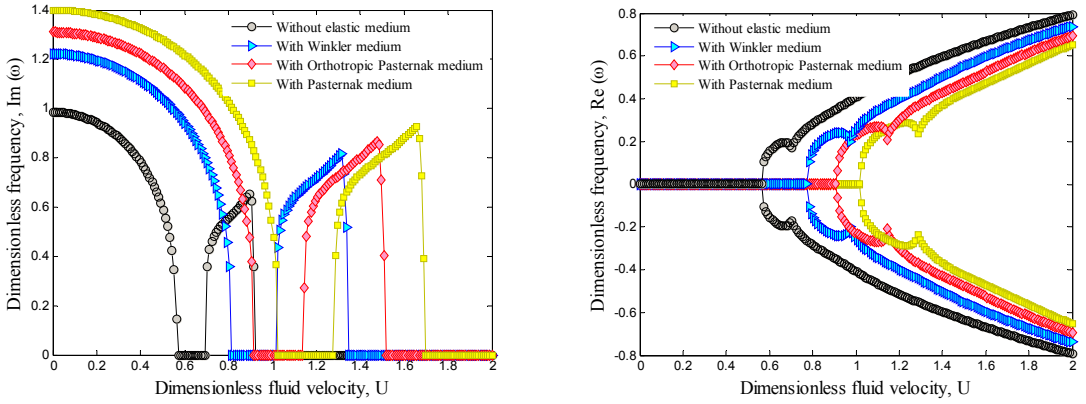

(a) (b)

Fig. 6 Effects of elastic medium type on the (a) dimension frequency (Im(ω)); (b) dimension frequency (Re(ω)) versus dimension flow velocity

Fig. 5 shows the volume percent of CNT on the frequency ration of system with respect to the maximum deflection. As can be seen, with increasing CNT volume percent, the frequency ratio decreases. In other words, the effects of nonlinear term in motion equation become lower. In addition, this effect on the frequency ration becomes more prominent at higher maximum deflection.

In order to show the effect of elastic foundation type, Figs. 6(a) and (b) are plotted. In this figure, four cases are considered namely as (I) without elastic medium, (II) Winkler medium, (III) orthotropic Pasternak medium and (IV) Pasternak medium. It is sown that the frequency and critical fluid velocity of system in the case of without elastic medium have minimum values since the stiffness of system is minimum. Furthermore, the effect of the Pasternak-type is higher than the Winkler-type on the natural frequency and critical fluid velocity of the sandwich structure. It is perhaps due to the fact that the Winkler-type is capable to describe just normal load of the elastic medium while the Pasternak-type describes both transverse shear and normal loads of the elastic medium. Meanwhile, the frequency and critical fluid velocity predicted by orthotropic Pasternak medium is lower that Pasternak medium since in orthotropic Pasternak medium, the angle of shear layer is considered 45.

Frequency ratio of sandwich structure is plotted in Fig. (7) against maximum amplitude for different elastic medium type. All of the results of Figs. 6(a) and (b) may be found in this figure. It is also concluded that neglecting elastic foundation, the effect of nonlinear terms on frequency of system become higher.

Figs. 8(a) and (b) show the dimensionless natural frequency and damping of the sandwich structure for different temperature gradients. As can be seen, the natural frequency and critical fluid velocity of the system decrease with increasing temperature. It is due to the fact that with increasing temperature gradient, the stiffness of system decreases.

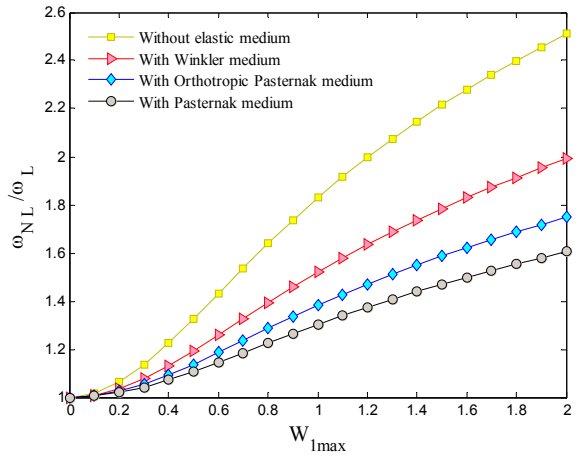

Fig. 7 Effects of elastic medium type on frequency ration versus maximum amplitude

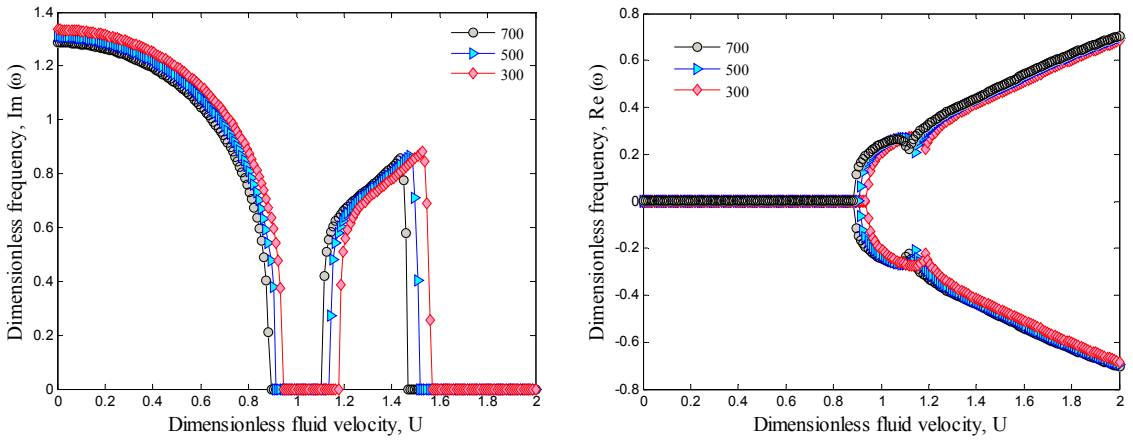

(a) (b)

Fig. 8 Effects of temperature gradient on the (a) dimension frequency (Im(ω)); (b) dimension frequency (Re(ω)) versus dimension flow velocity

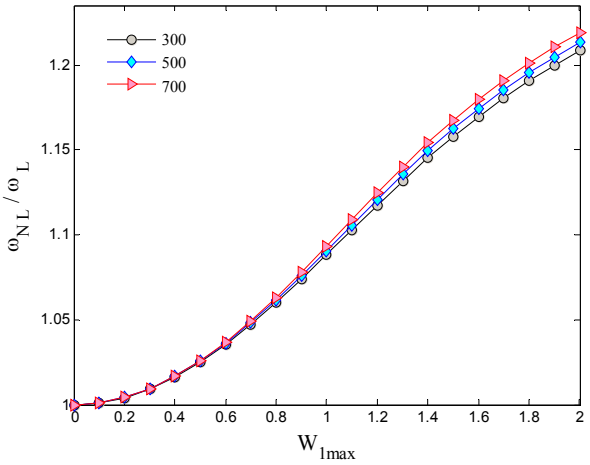

Fig. 9 Effects of temperature gradient on frequency ration versus maximum amplitude

Fig. 9 demonstrates the effect of temperature gradient on the frequency ration of sandwich structure. As can be seen, the effect of temperature gradient is very low with respect to other parameters. In addition, with increasing temperature gradient, the frequency ration increases due to decrease in stiffness of system.

6. Conclusions

Nonlinear vibration and instability of temperature-dependent piezoelectric coupled FG-CNTRC-cylindrical shell conveying viscous fluid based on the Mindlin theory were studied. Material properties of the CNTRC-cylindrical shells were assumed to be graded in the thickness direction and effective material properties were estimated by rule of mixture. The surrounding

elastic foundation was modeled with temperature-dependent orthotropic Pasternak foundation. Considering coupling of mechanical and electrical fields, the motion equations were derived based on Mindlin theory. Frequency and critical fluid velocity of sandwich structure were obtained based on DQM. The effects of the volume fractions of CNTs, distribution type of CNT, elastic medium and temperature were considered. Results indicate that FGO cylindrical shells have the lowest values of the non-dimensional frequency and the maximum values of the non-dimensional frequency occurs for FGX cylindrical shell. Furthermore, frequency and critical fluid velocity of the system increases with increasing volume fraction of CNTs since stiffness of sandwich structure increases when the CNT volume increases.

Acknowledgments

The authors are grateful to University of Kashan for supporting this work by Grant No. 363443/55. They would also like to thank the Iranian Nanotechnology Development Committee for their financial support.

References

Benrahou, W.T.K.H., Houari, M.S.A. and Tounsi, A. (2015), "Thermal buckling analysis of FG plates resting on elastic foundation based on an efficient and simple trigonometric shear deformation theory", *Steel Compos. Struct., Int. J.*, **18**(2), 443-465.

Cao, L., Mantell, S. and Polla, D. (2001), "Design and simulation of an implantable medical drug delivery system using microelectromechanical systems technology", *Sens. Act. A*, **94**(1-2), 117-125.

Chee, C.Y.K., Tong, L. and Steve, G.P. (1998), "A review on the modeling of piezoelectric sensors and actuators incorporated in intelligent structures", *J. Intel. Mat. Sys. Struct.*, **9**(1), 3-19.

Chen, X., Fox, C.H.J. and McWilliam, S. (2004), "Optimization of a cantilever microswitch with piezoelectric actuation", *J. Intel. Mat. Sys. Struct.*, **15**(11), 823-834.

Chen, W.Q., Jin, P.J. and Kang, Y.L. (2006), "Static and dynamic behavior of simply-supported cross-ply laminated piezoelectric cylindrical panels with imperfect bonding", *Compos. Struct.*, **74**(3), 265-276.

Clark, R.L. and Fuller, C.R. (1991), "Active control of structurally radiated sound from an enclosed finite cylinder", *Proceedings of the Conference on Recent Advances in Active Control of Sound and Vibration*, Virginia Polytechnic Institute and State University, Blacksburg, VA, USA, July.

Esawi, A.M.K. and Farag, M.M. (2007), "Carbon nanotube reinforced composites: potential and current challenges", *Mat. Des.*, **28**(9), 2394-2401.

Dong, S., Du, X., Bouchilloux, P. and Uchino, K. (2002), "Piezoelectric ring-morph actuation for valve application", *J. Electrocer.*, **8**(2), 155-161.

D'Ottavio, M., Ballhause, D., Kröplin, B. and Carrera, E. (2006), "Closed-form solutions for the free-vibration problem of multilayered piezoelectric shells", *Comput. Struct.*, **84**(22-23), 1506-1518.

Ghorbanpour Arani, A., Vossough, H., Kolahchi, R. and Mosallaie Barzoki, A.A. (2012), "Electro-thermo nonlocal nonlinear vibration in an embedded polymeric piezoelectric micro plate reinforced by DWBNNTs using DQM", *J. Mech. Sci. Tech.*, **26**(10), 3047-3057.

Ghorbanpour Arani, A., Kolahchi, R. and Khoddami Maraghi, Z. (2013), "Nonlinear vibration and instability of embedded double-walled boron nitride nanotubes based on nonlocal cylindrical shell theory", *Appl. Math. Model.*, **37**(14-15), 7685-7707.

Ghorbanpour Arani, A., Abdollahian, M. and Kolahchi, R. (2015), "Nonlinear vibration of embedded smart composite microtube conveying fluid based on modified couple stress theory", *Polym. Compos.*, **36**(7), 1314-1324. DOI: 10.1002/pc.23036.

Kutlu, A. and Omurtag, M.H. (2012), "Large deflection bending analysis of elliptic plates on orthotropic elastic foundation with mixed finite element method", *Int. J. Mech. Sci.*, **65**(1), 64-74.
Lester, H.C. and Lefebvre, S. (1991), "Piezoelectric actuator models for active sound and vibration control of cylinders", *Proceedings of the Conferenceon Recent Advances in Active Control of Sound and Vibration*, Virginia Polytechnic Institute and State University, Blacksburg, VA, USA, July.
Li, H., Lin, Q., Liu, Z. and Wang, C. (2001), "Free vibration of piezoelastic laminated cylindrical shells under hydrostatic pressure", *Int. J. Solids Struct.*, **38**(42-43), 7571-7585.
Lin, S. (2004), "Study on the equivalent circuit and coupled vibration for the longitudinally polarized piezoelectric ceramic hollow cylinders", *J. Sound Vib.*, **275**(3-5), 859-875.
Lu, P., Lee, K.H., Lin, W.Z. and Lim, S.P. (2001), "An approximate frequency formula for piezoelectric circular cylindrical shells", *J. Sound Vib.*, **242**(2), 309-320.
Moon, K., Seok, H. and Moonsan, J. (2009), "Dynamic modeling and active vibration controller design for a cylindrical shell equipped with piezoelectric sensors and actuators", *J. Sound Vib.*, **321**(3-5), 510-524.
Najafov, A.M., Sofiyev, A.H., Hui, D., Karaca, Z., Kalpakci, V. and Ozcelik, M. (2014), "Stability of EG cylindrical shells with shear stresses on a Pasternak foundation", *Steel Compos. Struct., Int. J.*, **17**(4), 453-470.
Reddy, J.N. (1984), "A simple higher order theory for laminated composite plates", *J. Appl. Mech.*, **51**(4), 745-752.
Santos, H., Soares, C.M.M., Soares, C.A.M. and Reddy, J.N. (2008), "A finite element model for the analysis of 3D axisymmetric laminated shells with piezoelectric sensors and actuators: Bending and free vibrations", *Comput. Struct.*, **86**(9), 940-947.
Shen, H.S. (2009), "Nonlinear bending of functionally graded carbon nanotube-reinforced composite plates in thermal environments", *Compos. Struct.*, **91**(1), 9-19.
Siao, J.C.T., Dong, S.B. and Song, J. (1994), "Frequency spectra of laminated piezoelectric cylinders", *ASME J. Vib. Acoust.*, **116**(3), 364-370.
Sohn, J.W., Kim, H.S. and Choi, S.B. (2006), "Dynamic modeling and vibration control of smart hull structure", *Trans. Korean Soc. Noise Vib. Eng.*, **16**(8), 840-847.
Spencer, W.J., Corbett, W.T., Dominguez, L.R. and Shafer, B.D. (1978), "An electronically controlled piezoelectric insulin pump and valves", *IEEE*, **25**(3), 153-156.
Vel, S.S. and Baillargeon, B.P. (2005), "Analysis of static deformation, vibration and active damping of cylindrical composite shells with piezoelectric shear actuators", *J. Vib. Acoust.*, **127**(4), 395-407.
Wang, L. and Ni, Q. (2009), "A reappraisal of the computational modelling of carbon nanotubes conveying viscous fluid", *Mech. Res. Commun.*, **36**(7), 833-837.

CC